Mechanism and Kinetics of Merocyanine 540 Binding to Phospholipid Membranes†

A. S. Verkman

Department of Medicine and Division of Nephrology, Cardiovascular Research Institute, University of California, San Francisco, California 94143

Received November 17, 1986; Revised Manuscript Received February 12, 1987

ABSTRACT: The physicochemical mechanism for merocyanine 540 (M540) binding to unilamellar phosphatidylcholine (PC) vesicles was examined by steady-state and dynamic fluorescence and fluorescence stopped-flow methods. At 530-nm excitation, aqueous M540 has an emission peak at 565 nm, which red shifts to 580 nm with formation of membrane-bound monomers (M); bound dimers (D) are nonfluorescent. Equilibrium fluorescence titrations show that 50% of total M540 partitions into the membrane to form D at [M540]/[PC] ($R_{m/p}$) $\sim$ 0.6. M and D concentrations are equal at $R_{m/p} \sim 0.05$. For $R_{m/p} < 0.1$, M540 has a single fluorescence lifetime (τ), which decreases with $R_{m/p}$ [τ^{-1} (ns^{-1}) = 0.48 + 3.3$R_{m/p}$], indicating a rapid collisional rate between M to form D. Dynamic depolarization studies show that hindered rotation of M (r_∞ = 0.13 at $R_{m/p}$ = 0.006) becomes more rapid (rotational rate 0.2–1.9 ns^{-1}) with increasing $R_{m/p}$ (0.006–0.075). The efficiencies of energy transfer between *n*-(9-anthroyloxy) fatty acid probes (*n* = 2, 6, 9, 12, 16) and bound M540 suggest that M is oriented parallel to the phospholipids near the membrane surface; studies of efficiencies of *n*-AF quenching by D are consistent with an orientation of D perpendicular to the phospholipids. In stopped-flow fluorescence measurements in which M540 is mixed with PC vesicles, there is a rapid (1 ms) followed by a slower (10–50 ms) concentration-dependent fluorescence increase. Taken together with previous temperature-jump results [Verkman, A. S., & Frosch, M. P. (1985) *Biochemistry 24*, 7117–7122], these data suggest that solution M540 binds to the PC vesicle membrane in <1 ms to a position parallel to the phospholipids where it undergoes 90° reorientation in $\sim$1 ms and dimerization in <10 ns to lie perpendicular to the phospholipids deep in the membrane. M540 then undergoes a 10-ms translocation to a site at the opposite membrane surface.

Merocyanine 540 (M540) is a widely used potential-sensitive optical dye. The absorbance and fluorescence of M540 respond rapidly (<1 ms) to changes in transmembrane electrical potential. M540 has been used to measure rapid potential transients in nerve and muscle cells (Davila et al., 1973; Senseman et al., 1983; Hirota et al., 1985) and steady-state potentials in cell and vesicle suspensions (Kinnally et al., 1978; Haeyaert & Verdonck, 1979; Smith et al., 1984). In addition, M540 has been used as a marker for altered cell differentiation and metaplasia on the basis of the sensitivity of M540 binding to changes in membrane phospholipid content and zeta potential (Reed et al., 1985; Kass, 1986).

The physicochemical mechanism of M540 binding to phospholipid membranes and the response mechanism of M540 to changes in transmembrane potential have been addressed in a number of studies (Ross et al., 1974; Tasaki & Warashina, 1976; Waggoner & Grinvald, 1977; Ross et al., 1977; Dragsten & Webb, 1978; Lelkes & Miller, 1980; Wolf & Waggoner, 1986). Measurements of M540 absorption and fluorescence spectra in squid axon and hemispherical lipid bilayers showed that a shift in the equilibrium between bound M540 fluorescent monomers and nonfluorescent dimers occurred when membrane potential was changed (Ross et al., 1974; Dragsten & Webb, 1978). It was suggested that dimers formed upon 90° rotation of a monomer positioned with axis perpendicular to the plane of the membrane. Recently we used the temperature-jump technique to examine the mechanism and rapid kinetics of M540 interaction with single-walled phosphatidylcholine (PC) vesicles (Verkman & Frosch, 1985). The data supported a reorientation–dimerization mechanism with a rate constant for M540 rotation from a position parallel to perpendicular to the plane of the membrane of 1340 s^{-1}; dimerization occurred in under 5 μs.

We report here a series of fluorescence studies designed to examine the interaction mechanism of M540 with PC vesicles and the location of the M540 binding site. Steady-state fluorescence measurements are used to define M540-PC vesicle equilibrium affinities. Phase-modulation lifetime and polarization measurements are used to study nanosecond M540 rotation and dimerization kinetics. The M540 binding site is localized from the efficiencies of energy transfer between *n*-(9-anthroyloxy) fatty acids (*n*-AF) and M540 and the quenching of *n*-AF fluorescence by M540. Finally, fluorescence stopped-flow is used to study millisecond kinetics processes of M540 binding to PC vesicles that were not measureable by the temperature-jump technique. The results are incorporated into a stepwise mechanism for M540 binding to PC vesicles to serve as a basis upon which to examine effects of membrane potential and phospholipid composition on M540 fluorescence in artificial and biological membranes.

Materials and Methods

Materials. M540 and the *n*-AF probes [2-, 6-, 9-, and 12-(9-anthroyloxy)stearic acids and 16-(9-anthroyloxy)palmitic acid] were purchased from Molecular Probes Inc. (Junction City, OR). M540 was added from a freshly prepared 1 mM aqueous stock solution kept in the dark at 4 °C; *n*-AF probes were added from 1 mM stock solutions in ethanol stored at −70 °C. All other chemicals were obtained from Sigma Chemical Co. (St. Louis, MO).

Vesicle Preparation. Unilamellar egg phosphatidylcholine (PC) vesicles were prepared by probe sonication of $\sim$25 mM PC at 4 °C under N_2 on a Microson MS-50 cell disruptor (Heat Systems-Ultrasonics Inc., Farmingdale, NY) (Huang & Thompson, 1974). Buffer consisted of 100 mM Tris–maleate and 100 mM KCl, pH 7.4. Vesicles were centrifuged

†Supported by grants from the National Institutes of Health (AM35124), the University of California, San Francisco Academic Senate, and the Hedco Foundation.

0006-2960/87/0426-4050$01.50/0

at 50000*g* for 45 min to remove multilamellar vesicles and titanium particles. Vesicles were stored under N_2 at 4 °C and used within 48 h of preparation. Lipid concentration was assayed by the method of Gomori (1942).

Stopped-Flow Experiments. Stopped-flow measurements were performed on a Dionex 130 stopped-flow apparatus (Sunnyvale, CA) interfaced to a MINC/23 computer (Digital Equipment Corp., Maynard, MA). The instrument dead time was <2 ms, and the maximum rate of data acquisition was 80 μs/point. The excitation wavelength was 530 nm as set by a Zeiss double monochromator; emission light was filtered by a Corion 595 cut-on filter.

Steady-State Fluorescence Experiments. Steady-state fluorescence intensity and anisotropy measurements were performed on an SLM 8225 fluorometer (Urbana, IL) using photon counting detection. Excitation light was set by a double monochromator; emission was measured by a single monochromator. Anisotropy was measured with Glan-Thompson polarizers in the L-format with correction for scattered light (generally <1%). Steady-state intensities were measured with a vertical excitation polarizer and emission polarizer oriented at 57.4° from the vertical. All measurements were performed at 23 °C with a thermostated cuvette holder and circulating water bath.

For *n*-AF studies, microliter quantities of *n*-AF stock solution were added to a stirred cuvette containing PC vesicles to give a dye to lipid ratio of 1:100. Vesicles were incubated 1 h with *n*-AF at 23 °C after which time fluorescence was stable. Under these conditions <1% of measured fluorescence arose from aqueous *n*-AF. For *n*-AF quenching studies, excitation and emission wavelengths were 365 and 435 nm.

Phase-Modulation Fluorescence Experiments. Fluorescence lifetime and dynamic depolarization measurements were performed on an SLM 4800 fluorimeter interfaced to an IBM PC/XT computer as described previously (Cabrini & Verkman, 1986a). Excitation light (530 nm) was selected with a monochromator, and emission light was filtered by Schott 595-nm sharp cut-on filters. For lifetime studies, an isochronal reference solution was used (Barrow & Lentz, 1983) consisting of M540 in ethylene glycol. The phase lifetimes of 3 μM M540 in ethylene glycol were 0.89 ns (30 MHz), 0.88 ns (18 MHz), and 0.91 ns (6 MHz) measured against a dilute glycogen reference solution. The mean lifetime, 0.90 ns, did not vary with M540 concentration (0–20 μM). Sample and reference intensities were matched to within 5% in all measurements. Ground-state heterogeneity analysis of phase and modulation lifetimes obtained at 6-, 18-, and 30-MHz modulation frequencies were performed with a gradient/grid fitting procedure described previously (Illsley et al., 1987). For lifetime measurements of *n*-AF probes in PC vesicles, the excitation wavelength was 365 nm and emitted light was measured at the blue end of the spectrum to minimize effects of excited-state reaction kinetics using a 420 ± 10 nm interference filter. The reference solution consisted of 1,4-bis(4-methyl-5-phenyloxazol-2-yl)benzene [$(Me)_2$POPOP] in ethanol (lifetime 1.45 ns).

Anisotropy decay experiments were performed by differential phase fluorimetry at 30-MHz modulation frequency using the T-format. M540 rotation rate (R) and limiting anisotropy (r_∞) were calculated from measured M540 steady-state anisotropy (r), lifetime (τ), and differential tangent (tan Δ) with equations developed for isotropic rotation of a single hindered fluorophore (Lakowicz et al., 1979).

Results

The studies are designed to establish (1) equilibrium binding characteristics of M540 in PC vesicles, (2) the location and motional dynamics of M540 in its binding sites, and (3) the kinetics of M540 interactions with the membrane. Steady-state fluorescence binding data will be presented first to define the aqueous and bound forms of M540. M540 motional dynamics will be studied with use of phase-modulation fluorescence, and bound M540 will be localized from *n*-AF fluorescence energy transfer and quenching. Kinetic studies will be performed by stopped-flow fluorescence.

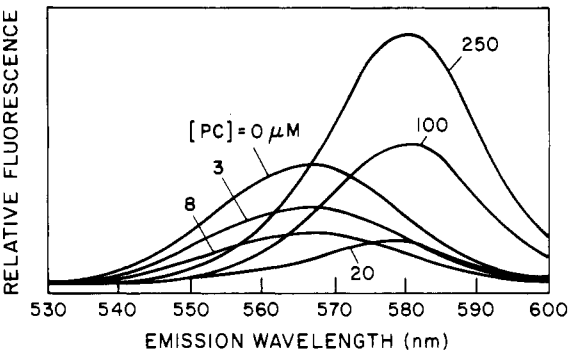

FIGURE 1: Fluorescence spectra of M540 in PC vesicles. Solutions consist of 3 μM M540 in 100 mM KCl and 100 mM Tris–maleate, pH 7.4, 23 °C containing specified concentrations of PC in unilamellar vesicles. Fluorescence was excited at 490 nm with vertically polarized light (4-nm band-pass) and detected with a polarizer oriented at 57.4° from the vertical (4-nm band-pass).

Equilibrium Binding Measurements. Equilibrium fluorescence emission spectra for M540 binding to PC vesicles are shown in Figure 1. At constant M540 concentration (3 μM), addition of PC results first in a decrease in fluorescence at 565 nm as aqueous M540 partitions into the membrane to form nonfluorescent dimers and then in an increase in fluorescence at 580 nm as membrane-bound dimers are converted into fluorescent membrane-bound monomers. This interpretation is supported by previous studies suggesting that membrane-bound M540 exists in monomer and dimer forms (Ross et al., 1974; Tasaki & Warashina, 1976; Waggoner & Grinvald, 1977; Dragsten & Webb, 1978) and by studies of cyanine dye binding to biological membranes (Cabrini & Verkman, 1986a,b), where a similar series of spectra was obtained. On the basis of absorbance properties of M540, we showed previously that aqueous M540, bound dimer, and bound monomer had absorbance peaks at 540, 530, and 570 nm, respectively (Verkman & Frosch, 1985); estimated half-points for interconversion between aqueous M540 and bound dimer occurred at [M540]/[PC] of 0.5–1 and for interconversion between bound dimer and monomer at [M540]/[PC] of 0.05–0.1, similar to the fluorescence data.

The binding affinity for M540 to PC vesicles and the monomer–dimer equilibrium constants were quantitated from fluorescence titration data. Figure 2 (top) shows the decrease in fluorescence at 565 nm as aqueous M540 partitions into the membrane to form bound dimer. Data were fitted to a saturable, single-site binding model with K_{app}, the PC concentration at which 50% M540 binding occurs (Cabrini & Verkman, 1986a), of 5.2 μM (3 μM M540) and 9.4 μM (6 μM M540). The increase in K_{app} with [M540] indicates that saturable binding occurs with at least one dimer bound for every three PC molecules; however, exact determination of total site stoichiometry and binding affinity is not easily accomplished from titration data alone. Figure 2 (bottom) shows the increase in fluorescence at 580 nm with conversion between bound dimers and monomers. Because the monomer–dimer equilibrium depends only on the two-dimensional density of M540 molecules (Verkman & Frosch, 1985), the dimerization

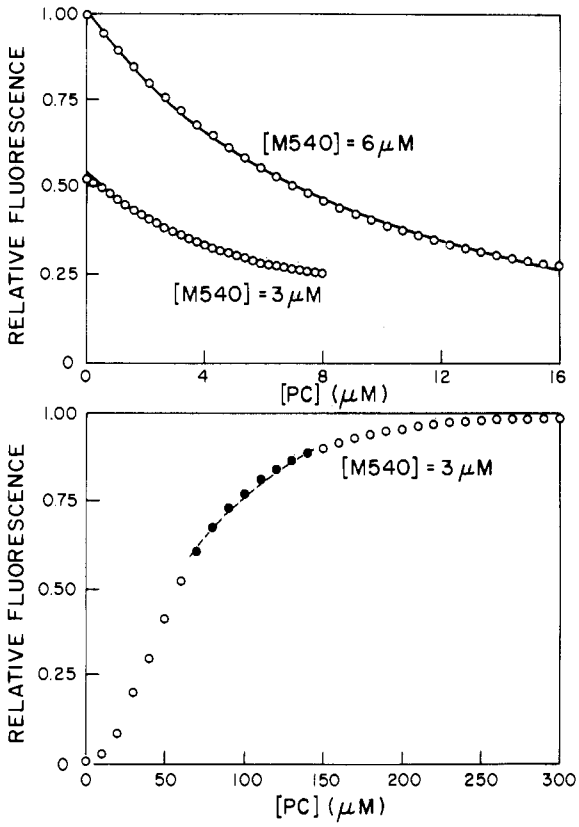

FIGURE 2: Equilibrium binding of M540 to PC vesicles. Solutions consist of specified M540 and PC concentrations in 100 mM KCl and 100 mM Tris–maleate, pH 7.4, 23 °C. Titration curves were obtained by adding microliter quantities of a PC vesicle suspension to a stirred cuvette containing M540. Each curve is one experiment typical of two. Top: Fluorescence was excited at 490 nm and monitored at 565 nm (4-nm band-pass). Data were fitted to a single site saturable binding model: $F_{565} = F_0 - F_\infty[PC]/(K_{app} + [PC])$, where F_0 and F_∞ are F_{565} in the absence and presence of maximum PC with $K_{app} = 5.2 \pm 0.3$ μM ([M540] = 3 μM) and 9.4 ± 0.4 μM ([M540] = 6 μM). Bottom: Fluorescence was excited at 530 nm and monitored at 590 nm (4-nm band-pass). Data points in which monomer–dimer equilibration occurs primarily (filled circles) were fitted to the dimerization equation derived previously [Cabrini and Verkman (1986a) eq A5] with $K_d = 0.034 \pm 0.008$.

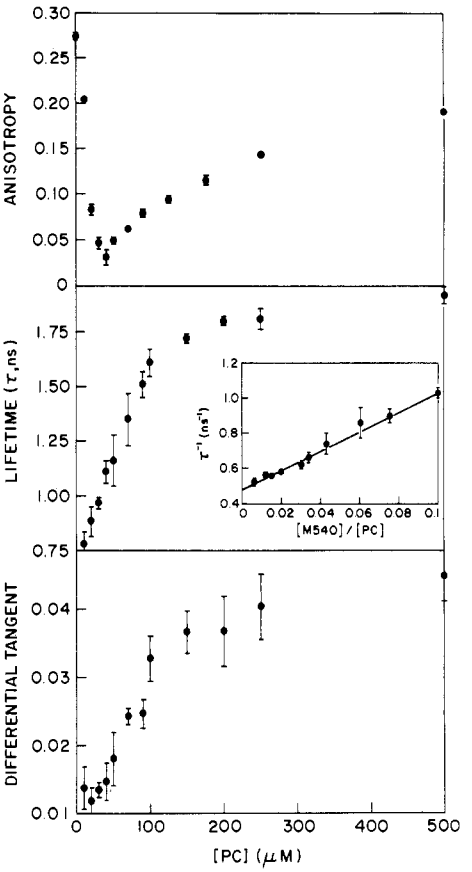

FIGURE 3: Lifetime and polarization studies of M540 binding to PC vesicles. Solutions consist of 3 μM M540 and specified concentrations of PC vesicles in 100 mM KCl and 100 mM Tris–maleate, pH 7.4, 23 °C. Each data point is the mean ± SD of measurements performed in quadruplicate. Top: Steady-state anisotropy was determined in the L-format with excitation at 530 nm and emission at 590 nm. Middle: Fluorescence phase and modulation lifetimes were measured by phase-modulation methods at 6-, 18-, and 30-MHz modulation frequencies with excitation at 530 nm and emission at >595 nm. A ground-state heterogeneity analysis indicated the presence of a single lifetime (fractional amplitude >0.98) for [PC] > 30 μM ([M540]/[PC] < 0.1). For [PC] = 10–30 μM the lifetime of the major component (92–98%) is plotted. Inset: The same data are plotted as reciprocal fluorescence lifetime vs. [M540]/[PC]. Linear regression gives slope 3.3 ± 0.2 ns^{-1} and intercept 0.475 ± 0.005 ns^{-1}. Bottom: The differential tangent was determined in the T-format at a 30-MHz modulation frequency with excitation at 530 nm and emission at >595 nm.

constant, K_d, is the dimensionless quantity $[C_M]^2/([C_D]/[PC])$ where C_M and C_D are monomer and dimer concentrations in the total solution (μM). The fluorescence data in Figure 2 (bottom) were fitted to an intramembrane dimerization model (Cabrini & Verkman, 1986a) with $K_d = 0.034$, similar to the reported value of 0.06 determined by an independent absorbance method (Verkman & Frosch, 1985).

Several additional spectral studies were performed to characterize the fluorescence properties of aqueous and bound M540. For aqueous M540, the shape of the fluorescence and absorbance spectra and the fluorescence anisotropies and lifetimes were independent of concentration (0–20 μM), indicating absence of M540 dimerization in solution at M540 concentrations used in these measurements. For both aqueous M540 and the bound monomer, the shapes of emission spectra were independent of excitation wavelength (450–570 nm) and the shapes of the excitation spectra were independent of emission wavelength (540–600 nm). The M540 excitation spectrum was broad, with a gradual increase in intensity as wavelength increased between 430 and 570 nm (not shown); the spectral shape was independent of PC concentration.

Time-Resolved Fluorescence Measurements. Phase-modulation fluorescence studies were performed to examine the kinetics of intramembrane M540 dimerization and the rotational dynamics of bound M540. Using the temperature-jump technique we showed previously that while monomer reorientation from a position perpendicular to parallel to the phospholipid chains occurred in ~1 ms, the dimerization reaction occurred in <4 μs, the resolution time of the temperature-jump method (Verkman & Frosch, 1985). Assuming a diffusion coefficient of 10^{-6} cm/s for membrane-bound M540 monomer, it was estimated that the mean time between M540–M540 collisions would be 1–10 ns as [M540]/[PC] varies between 0.1 and 0.01. It is thus predicted that the M540 fluorescence lifetime should be dependent upon [M540]/[PC].

Figure 3 (middle) shows the dependence of M540 lifetime on PC concentration at 3 μM M540. Interestingly, for [PC] > 30 μM ([M540]/[PC] < 0.1) a single lifetime was observed as judged by a ground-state heterogeneity analysis using phase and modulation lifetime data measured at three modulation frequencies. At a fixed [M540]/[PC] < 0.1 the lifetime was independent of [M540] (1–6 μM, data not shown) and emission wavelength (560–610 nm using emission monochromator, 16-nm band-pass). These results suggest that the

Table I: Rotational Characteristics of M540 in PC Vesicles[a]

[M540]/[PC]	R (ns^{-1})	r_∞	cone angle (deg)
0.075	1.9 ± 0.4	0.0047 ± 0.0002	79.0
0.06	1.4 ± 0.4	0.017 ± 0.001	70.9
0.043	0.97 ± 0.2	0.023 ± 0.002	68.0
0.033	0.90 ± 0.1	0.045 ± 0.008	61.5
0.03	0.65 ± 0.07	0.036 ± 0.001	63.8
0.02	0.51 ± 0.04	0.056 ± 0.002	58.6
0.015	0.47 ± 0.07	0.073 ± 0.002	55.1
0.012	0.36 ± 0.05	0.088 ± 0.002	52.2
0.006	0.23 ± 0.02	0.127 ± 0.002	45.6

[a] Solutions consist of 3 μM M540 with variable [PC] in 100 mM KCl and 100 mM Tris–maleate, pH 7.4, 23 °C. M540 rotational rate (R), limiting anisotropy (r_∞), and cone angle were calculated from anisotropy, lifetime, and tan Δ given in Figure 3, assuming that M540 is an isotropic hindered rotator (Lakowicz et al., 1979). M540 anisotropy in the absence of depolarizing rotations (r_0) was taken to be 0.36 on the basis of the measured anisotropy of 3 μM M540 in lauryl alcohol and in 2 M sucrose at 4 °C. Errors (SD) in R and r_∞ were obtained by propagation of errors in anisotropy, lifetime, and tan Δ.

M540 fluorescence lifetime is dependent upon M540 density in the membrane, and thus upon the collisional rate of M540 in its excited state (M540*) with ground-state M540. If k_r is the rate of radiative decay of M540* and if k_{nr}[M540]/[PC] is the rate of nonradiative decay (assuming all membrane-bound M540 can quench M540* fluorescence), then a plot of reciprocal lifetime vs. [M540]/[PC] should be linear with slope k_{nr} and intercept k_r. The inset to Figure 3 is consistent with this interpretation; the slope 3.3 ns^{-1} predicts that the M540 collisional time should be ~3 ns for [M540]/[PC] = 0.1, similar to the estimates given above. These measurements provide information about the collisional frequency and lateral diffusibility of M540; determination of a bimolecular rate constant for dimerization would require knowledge of reaction efficiency, which is not available.

Steady-state and dynamic depolarization measurements were performed to measure rapid rotations of membrane bound M540. The steady-state anisotropy of M540 decreases and then increases with increasing [PC] (Figure 3, top). The initial decrease is due to coexistence of aqueous M540 (anisotropy 0.27) and bound monomer. This interpretation is supported by anisotropy spectra in which anisotropy varied from 0.27 to <0.05 with increasing emission wavelength (550–600 nm) for [PC] < 30 μM. For [PC] > 50 μM the anisotropy was independent of emission wavelength, supporting the presence of a single M540 fluorescent species as predicted from binding and lifetime measurements.

To determine whether the increased anisotropy was due to changes in M540 lifetime or in M540 rotational characteristics, differential tangents (tan Δ) were measured (Figure 3, bottom). Table I summarizes the rotational rates (R), limiting anisotropies (r_∞), and cone angles calculated from measured anisotropy, lifetime, and tan Δ data, assuming that M540 rotation can be described by the formalism developed for isotropic rotations of a single hindered fluorophore (Lakowicz et al., 1979). The results indicate a marked increase in apparent M540 rotational rate with increased [M540]/[PC], suggesting either that the lipid bilayer is perturbed at high [M540]/[PC] or that radiative energy transfer increases R when donor and acceptor M540 are nonparallel. The increase in calculated cone angle indicates that M540 motion is less hindered with increasing [M540]/[PC], again a finding consistent with either lipid perturbation or energy transfer. Another possible interpretation of these results is that rotation of M540 in the bilayer is anisotropic and that the degree of anisotropy depends upon [M540]. Measurement of multifrequency differential-phase and modulation lifetimes would help to distinguish among these possibilities.

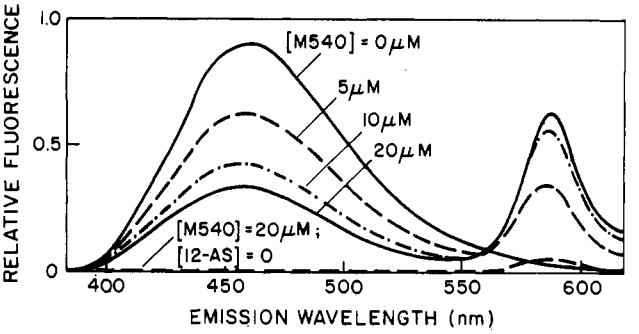

FIGURE 4: Energy transfer between 12-AS and M540 in PC vesicles. Solutions consist of 200 μM PC containing 0.5 μM 12-AS with specified M540 concentrations. Fluorescence was excited at 365 nm; 4-nm band-pass was used for excitation and emission monochromators. The dashed emission spectra labeled [M540] = 20 μM; [12-AS] = 0 was measured with use of 200 μM PC and 20 μM M540 without 12-AS.

Localization of M540 Binding Site. The equilibrium binding and phase-modulation fluorescence studies give information about M540 binding isotherms and rapid motional characteristics, but no information about the location and geometry of M540 binding sites. To localize M540 in the PC vesicle membrane, we use the *n*-AF probes, a series of lipophilic compounds with anthoyloxy fluorophores located at graded depths within the transverse plane of the bilayer (Blatt & Sawyer, 1985). These probes have been used to define the binding positions of a number of molecules including the membrane-potential-sensitive cyanine dyes (Cabrini & Verkman, 1986c). Two approaches will be used to localize M540: *n*-AF to M540 energy transfer and quenching of *n*-AF fluorescence by M540. Energy-transfer measurements give information only about fluorescent M540 monomers, whereas quenching measurements give information about both monomers and dimers.

Figure 4 shows the emission spectra for 12-AS and M540 incorporated into PC vesicle membranes. At an excitation wavelength of 360 nm there is very little direct excitation of M540 (dashed curve labeled [M540] = 20 μM; [12-AS] = 0). In the presence of 12-AS and with increasing [M540], there is quenching of donor (12-AS) fluorescence with appearance of an M540 peak at 580 nm due to radiative energy transfer. Similar series of spectra were obtained with use of 2-AS, 6-AS, 9-AS, and 16-AP in place of 12-AS. The efficiency of energy transfer is dependent upon overlap of donor emission and acceptor excitation spectra, donor–acceptor orientation, and the distance between donor and acceptor (Stryer, 1978). Because the spectral shape of *n*-AF emission is almost independent of *n* and because the M540 peak height at 580 nm is approximately proportional to the integrated area of the energy-transfer peak, the ratio of the peak height at 580 nm (with subtraction of the small contribution from direct M540 excitation) to the peak height at 465 nm measured in the absence of M540 (F_{580}/F_{465}) is a semiquantitative measure of energy-transfer efficiency and thus of spatial separation between donor and acceptor. At 20 μM M540, F_{580}/F_{465} is 0.92, 0.74, 0.60, 0.65, and 0.57 for n = 2, 6, 9, 12, and 16, respectively; similar sequences were obtained at 5 and 10 μM M540. Because the efficiency of energy transfer varies with the reciprocal sixth power of the distance between donor and acceptor, the presence of similar degrees of energy transfer for all *n* suggests that the M540 monomer is oriented parallel to the phospholipid chains and thus can interact with the

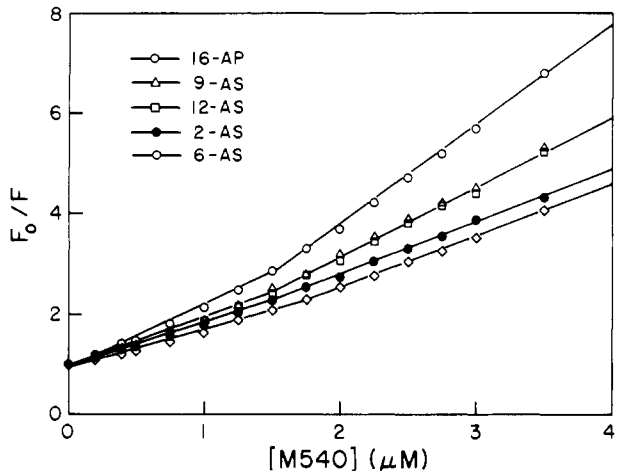

FIGURE 5: Stern–Volmer plot for quenching of *n*-AF probes by M540. Solutions consist of 50 μM PC containing 0.5 μM *n*-AF and increasing concentrations of M540. The ratio of fluorescence in the absence (F_0) to that in the presence (F) of M540 is plotted on the ordinate. Data were fitted to connected lines by a four-parameter nonlinear regression. At [M540] > 5 μM (not shown) the curves become concave downward and nearly independent of [M540]. At 20 μM M540, F_0/F is 6.2, 6.1, 7.6, 7.7, and 9.9 for n = 2, 6, 9, 12, and 16, respectively.

anthroyloxy group at all levels within the membrane. The decrease in F_{580}/F_{465} with increasing n suggests that the tip of the monomer lies very near the membrane surface.

The validity of this conclusion rests on the assumption that the position of *n*-AF does not change in the presence of M540 and that M540 does not bind directly to the anthroyloxy group. To examine these possibilities, the lifetimes of 12-AS were measured with increasing [M540]. For 100 μM PC containing 1 μM 12-AS, phase lifetimes at 18 MHz were 6.7, 5.0, 4.1, 3.2, and 2.7 ns for [M540] = 0, 1, 2, 3, and 4 μM, respectively. Formal heterogeneity analysis of phase and modulation lifetime data was not performed because the *n*-AF compounds undergo an excited-state reaction (Matayoshi & Kleinfeld, 1981). However, on the basis of the trend of decreasing 12-AS lifetime with increasing [M540], it is concluded that M540 quenches 12-AS fluorescence primarily by a collisional mechanism, which does not involve formation of an M540/12-AS static complex.

It is also assumed that the orientation between the anthroyloxy emission dipole and the M540 excitation dipole is random or is at least independent of n. The former assumption is commonly made in energy-transfer measurements using the *n*-AF probes. Finally, the interpretation of F_{580}/F_{465} as a distance parameter requires that the degree of nonradiative quenching of *n*-AF by M540 dimers be relatively independent of n so that the contribution of the *n*-AF emission spectrum to the overlap integral remain proportional to F_{465}. The quenching experiments below support this assumption.

The location of the M540 membrane-bound dimer was examined from the quenching of *n*-AF probes. The Stern–Volmer analysis is shown in Figure 5. In contrast to the sequence of efficiencies for energy transfer between *n*-AF and the M540 monomer, the order of efficiencies for *n*-AF quenching by M540 are $n = 16 \gg 12 \sim 9 > 2 \sim 6$. For [M540] > 2 μM, the predominent form of M540 is the dimer. The increased efficiencies for *n*-AS quenching by M540 as n increases suggest that the dimer resides deep within the membrane. Because M540 is quite long (~16 Å), these findings are most consistent with an orientation for the M540 dimer perpendicular to the phospholipid chain, deep within the membrane. An alternative interpretation of the results,

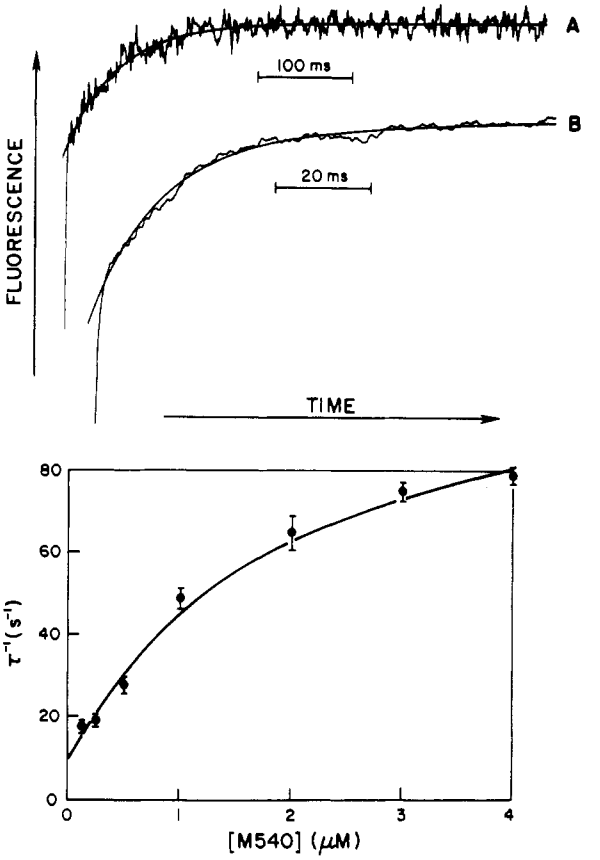

FIGURE 6: Stopped-flow kinetics of M540 binding to PC vesicles. Top: Stopped-flow time course of M540 interaction with PC vesicles. 100 μL of PC vesicles ([PC] = 50 μM) was mixed with an equal volume of M540 (A, 0.25 μM; B, 4 μM) in a stopped-flow apparatus at 23 °C. Fluorescence was excited at 530 nm and detected at >595 nm with use of a Corion cut-on filter. Fitted exponential time constants were 53 ms (A) and 14.2 ms (B). Bottom: Dependence of reciprocal exponential time constant on [M540]. Data points are mean ± SD for experiments performed in quadruplicate. Data were fitted to the saturable kinetic model of a bimolecular reaction followed by a rate-limiting unimolecular reaction: $\tau^{-1} = k_{-2} + k_2[M540]/(K_1 + [M540])$, with $k_{-2} = 9 \pm 3\ s^{-1}$, $k_2 = 106 \pm 10\ s^{-1}$, and $K_1 = 1.9 \pm 0.6\ \mu M$, where k_2 and k_{-2} are rate constants for the unimolecular reaction and K_1 is a dissociation constant for the bimolecular reaction.

which cannot be ruled out on the basis of the data presented, is that the location of M540 monomers or dimers becomes progressively deeper in the membrane as [M540]/[PC] increases due to lipid perturbation.

Stopped-Flow Kinetic Studies. Fluorescence stopped-flow measurements were performed to examine millisecond kinetic processes that were not measurable by the temperature-jump technique. Figure 6 (top) shows typical time courses of increasing fluorescence following rapid mixture of M540 with PC vesicles. At all M540 and PC concentration studies, the time course was biphasic. There was a rapid reaction with an exponential time constant of ~1 ms, which was obscured partially by the instrument dead time (1–2 ms). This was followed by a slower, single-exponential increase in fluorescence that depended upon M540 concentration (Figure 6, bottom), but not on PC concentration. At constant [M540] = 3 μM, exponential time constants were 10 ± 2, 10 ± 1, 11 ± 2, and 11 ± 2 ms for [PC] = 25, 50, 100, and 200 μM, respectively (data not shown). Although difficult to quantitate because of the instrument dead time, the ratio of amplitudes of the fast to slow exponential processes decreased ~5-fold with increasing [M540] (0.125–4 μM) at constant [PC] (50 μM). There were no slower reaction processes (100 ms–10 min) observed when M540 was mixed with PC vesicles in the

stopped-flow apparatus or in a fluorimeter cuvette.

The faster exponential reaction process has the same time constant as that measured for the M540 reorientation process characterized previously by the temperature-jump method. Because it was possible to observe a 1-ms reaction, the time constant for the initial bimolecular association of M540 with PC vesicles must be under 1 ms. In addition, it follows that the slower exponential reaction must occur after the 1-ms reaction. Temperature-jump and fluorescence lifetime data suggest that the slower reaction is not the dimerization process, which should occur in $\ll 1$ μs. Because the rate of the slower reaction saturates with increasing M540 concentration, this process is a rate-limiting unimolecular reaction, likely the translocation of M540 across the lipid bilayer, coupled to a faster bimolecular process (association or dimerization reactions). This interpretation is supported by the observation that the ratio of amplitudes of the fast to slow reactions decreases with increasing total [M540]; at low [M540], most of the [M540] partitions into the outer leaflet of the bilayer in <1 ms (fast reaction), resulting in relatively little further increase in fluorescence accompanying the unimolecular reaction. At high total [M540], there is adqeuate aqueous M540 to provide a large increase in fluorescence during the unimolecular reaction. The presence of a rate-limiting translocation process in the PC vesicle membrane is also supported by the relative independence of the slower exponential time constant on [PC] at high [M540].

Discussion

The mechanism for M540 interaction with a phospholipid membrane has been examined in a well-defined model system, unilamellar PC vesicles, using a combination of steady-state, phase-modulation, and kinetic fluorescence methods. These studies are an extension of our reported absorbance measurements of M540 relaxation kinetics in PC vesicle membranes by temperature-jump perturbations (Verkman & Frosch, 1985). The focus of the present study was to define physically the binding affinities and location, the motional characteristics, and the kinetics of M540 interaction with a homogeneous membrane system with a single buffer system in the absence of induced membrane potentials. These basic studies will be of utility in defining the mechanisms of M540 action in a number of different reported applications of M540 including measurements of membrane potential transients (Davila et al., 1973; Senseman et al., 1983), characterization of cell pathology on the basis of plasma membrane phospholipid composition and asymmetry (Reed et al., 1985; Kass, 1986), analysis of lipid domain structure (Lelkes & Miller, 1980; Williamson et al., 1983), and photosensitization of tumor cells (Meagher et al., 1983).

Our steady-state fluorescence studies define the interconversions between three forms of M540: a fluorescent aqueous monomer (emission peak 565 nm), a fluorescent membrane-bound monomer (emission peak 580 nm), and a nonfluorescent membrane-bound dimer. An intramembrane M540 monomer–dimer equilibrium was first proposed by Ross et al. (1974) and subsequently confirmed in several laboratories (Tasaki & Warashina, 1976; Ross et al., 1977; Dragsten & Webb, 1978; Waggoner & Grinvald, 1977), where it was suggested that M540 potential sensitivity resulted from electric field induced rotation of M540 monomers with consequent perturbation of the monomer–dimer equilibrium.

Energy-transfer experiments between the *n*-AF probes and M540 suggest that most of the fluorescent M540 monomers lie parallel to the phospholipid chains with the M540 sulfonate group probably near the membrane surface. From temperature-jump kinetic data it was calculated that at equilibrium there is a 5-fold excess of M540 monomers oriented parallel to phospholipids over those oriented in the perpendicular direction (parallel to the membrane surface) (Verkman & Frosch, 1985). Using polarization measurements in hemispherical lipid bilayers, Dragsten and Webb (1978) and, recently, Wolf and Waggoner (1986) provided evidence for the presence of three forms of membrane-bound M540, monomers oriented parallel and perpendicular to the phospholipids, and dimers oriented parallel to the phospholipids. Our results using an independent approach, fluorescence energy transfer and quenching of the depth-dependent *n*-AF fluorophores, support these proposed M540 orientations.

There must be at least four distinct kinetic processes that occur upon mixture of M540 with PC membranes: association, reorientation (rotation), dimerization, and translocation to the opposite leaflet of the membrane. In temperature-jump studies, we found that reorientation occurred in ~ 1 ms, whereas dimerization occurred within the instrument resolution time (4 μs). In the stopped-flow measurements reported here, the 1-ms reaction was observed, as well as a 10–50-ms exponential reaction process with increasing rate at increasing M540 concentrations. The dependences of the rate of the 10–50-ms process on [M540] and [PC] suggested that this process is a unimolecular reaction step, probably the translocation of M540 across the bilayer. It was also concluded that at [M540] between 0.125 and 4 μM the time constant for the initial association reaction is under 1 ms. Smith et al. (1980) used absorbance stopped-flow to study the binding kinetics of M540 to glycerylmonooleate suspensions and found a single concentration-independent time constant of ~ 10 ms at 5–30 μM M540, similar to the present data; however, they could not determine the physical nature of this pseudo-first-order reaction. The increased sensitivity of fluorescence over absorbance measurements allowed us to examine binding kinetics at low [M540], where the reaction rate was not saturated to its maximal value.

Phase-modulation fluorescence measurements provided information about the nanosecond kinetics of the dimerization reaction and the rotational mobility of the bound M540 monomer, which were too rapid to measure by temperature-jump or stopped-flow methods. Under conditions when virtually all M540 is membrane bound, a single fluorescence lifetime was observed that increased with increasing [M540]/[PC]. The data were interpreted in terms of a rapid (1–10-ns) collisional reaction between M540 in its excited state with ground-state M540. These results are consistent with the rapid dimerization rate measured in temperature-jump studies (<4 μs) and with the rapid response of M540 fluorescence to changes in transmembrane potential in hemispherical bilayer studies (Dragsten & Webb, 1978).

Acknowledgments

We thank David Sullivan for technical assistance.

References

Barrow, D. A., & Lentz, B. R. (1983) *J. Biochem. Biophys. Methods 7*, 217–234.

Blatt, E., & Sawyer, W. H. (1985) *Biochim. Biophys. Acta 822*, 43–62.

Cabrini, G., & Verkman, A. S. (1986a) *J. Membr. Biol. 90*, 163–175.

Cabrini, G., & Verkman, A. S. (1986b) *J. Membr. Biol. 92*, 171–182.

Cabrini, G., & Verkman, A. S. (1986c) *Biochim. Biophys. Acta 863*, 91–100.

Davila, H. V., Salzberg, B., Cohen, L. B., & Waggoner, A. S. (1973) *Nature (London), New Biol. 241*, 159-160.
Dragsten, P. R., & Webb, W. W. (1978) *Biochemistry 17*, 5228-5240.
Gomori, G. (1942) *J. Lab. Clin. Med. 27*, 955-960.
Haeyaert, P., & Verdonck, F. (1979) *Arch. Int. Phys. Biochem. 87*, 180-181.
Hirota, A., Kamino, K., Komuro, H., Sakai, T., & Yada, T. (1985) *J. Physiol. (London) 369*, 209-227.
Huang, C., & Thompson, T. E. (1974) *Methods Enzymol. 32*, 485-489.
Illsley, N. P., Lin, H. Y., & Verkman, A. S. (1987) *Biochemistry 26*, 446-454.
Kass, L. (1986) *Stain Technol. 61*, 7-15.
Kinnally, K. W., Tedeschi, H., & Maloff, B. L. (1978) *Biochemistry 17*, 3419-3428.
Lakowicz, J. R., Prendergast, F. G., & Hogen, D. (1979) *Biochemistry 18*, 508-519.
Lelkes, P. I., & Miller, I. R. (1980) *J. Membr. Biol. 52*, 1-15.
Matayoshi, E. D., & Kleinfeld, A. M. (1981) *Biophys. J. 35*, 215-235.
Meagher, R. C., Sieber, F., & Spivak, J. L. (1983) *J. Cell Physiol. 116*, 118-124.
Reed, J. A., Kough, R. H., Williamson, P. L., & Schlegel, R. A. (1985) *Cell Biol. Int. Rep. 9*, 43-49.
Ross, W. N., Salzberg, B. M., Cohen, L. B., & Davila, H. V. (1974) *Biophys. J. 14*, 983-986.
Ross, W. N., Salzberg, B. M., Cohen, L. B., Grinvald, A., Davila, H. V., Waggoner, A. S., & Wang, C. H. (1977) *J. Membr. Biol. 33*, 141-158.
Senseman, D. M., Shimizu, H., Horwitz, I. S., & Salzberg, B. M. (1983) *J. Gen. Physiol. 81*, 887-908.
Smith, J. C., Frank, S. J., Bashford, C. L., Chance, B., & Rudkin, B. (1980) *J. Membr. Biol. 54*, 127-139.
Smith, J. C., Graves, J. M., & Williamson, M. (1984) *Arch. Biochem. Biophys. 231*, 430-453.
Stryer, L. (1978) *Annu. Rev. Biochem. 47*, 819-846.
Tasaki, I., & Warashina, A. (1976) *Photochem. Photobiol. 24*, 191-207.
Verkman, A. S., & Frosch, M. P. (1985) *Biochemistry 24*, 7117-7122.
Waggoner, A. S., & Grinvald, A. (1977) *Ann. N.Y. Acad. Sci. 303*, 217-241.
Williamson, P., Mattocks, K., & Schlegel, R. A. (1983) *Biochim. Biophys. Acta 732*, 387-393.
Wolf, B. E., & Waggoner, A. S. (1986) *Soc. Gen. Physiol. Ser. 40*, 101-113.

Membrane Fusion Activity of Succinylated Melittin Is Triggered by Protonation of Its Carboxyl Groups

Masayuki Murata,[‡] Kuniaki Nagayama,[§] and Shun-ichi Ohnishi*[,‡]

Department of Biophysics, Faculty of Science, Kyoto University, Sakyo-ku, Kyoto 606, Japan, and Biometrology Lab Division, JEOL Ltd., Nakagami, Akishima, Tokyo 196, Japan

Received December 9, 1986; Revised Manuscript Received February 26, 1987

ABSTRACT: The membrane fusion activity of melittin and its succinylated derivative was studied as a function of pH by the transfer of spin-labeled phosphatidylcholine as well as by internal content mixing and electron microscopy. The protonation process of the carboxyl groups introduced into melittin was studied by ^{13}C NMR spectroscopy using the derivative prepared with [1,4-^{13}C]succinic anhydride. Melittin causes fusion of sonicated phosphatidylcholine vesicles in a wide range of pH. In marked contrast, melittin with all four amino groups succinylated induces fusion only at acidic pH lower than 5.2, with the maximum at pH 5.1. The fusion reactions are very rapid, reaching a saturation level within 1 min. The fusion efficiency depends on the peptide-to-phospholipid ratio in the reaction mixture. Trypsinized succinylated melittin, which has lost the four positively charged C-terminal residues, causes aggregation of vesicles at acidic pH but cannot induce fusion. The ^{13}C NMR peaks for the carboxyl and carbonyl groups of succinylated melittin shifted to higher field as the pH was lowered. The pK_a value of the four carboxyl groups was obtained as 5.19 and 4.83 in the presence and absence of vesicles, respectively. The pK_a value in the presence of vesicles agrees quite well with the half-maximal pH for fusion of 5.15, indicating that the fusion activity is triggered by protonation of the carboxyl groups in the hydrophobic segment of the peptide. The higher shift of pK_a value in the presence of vesicles can be due to stabilization of the protonated form by entrance into lipid bilayer hydrocarbon layer. Only a single peak was observed for each carboxyl and carbonyl group at various pH values, indicating fast exchange between the protonated and deprotonated forms of the segment, faster than the NMR time scale of 3 ms. If the protonated segment entered the lipid bilayer, the entrance and return to the surface of bilayer membrane should also be fast.

Membrane fusion plays an essential role in the intracellular sorted transport of materials in endocytic and exocytic processings of cells (Goldstein et al., 1986). It also provides an essential mechanism for enveloped viruses to transfer their genome into the target cell cytoplasm, a crucial initial step in infection. Elucidation of the mechanism of membrane fusions and their control is important for understanding the cellular processes.

Virus membrane fusions have been extensively studied, and

[‡] Kyoto University.
[§] JEOL Ltd.

0006-2960/87/0426-4056$01.50/0